A 3D modeling study on multi-layer distribution and formation mechanism of electrical charging in a severe thunderstorm

Zhimin Zhou[1,2] , and Xueliang Guo[1,3]

1 Zhimin Zhou, Institute of Heavy Rain CMA, Wuhan, Wuhan City, Hubei Province, China,430074

2 Graduate school of Chinese Academy of ScienCe, Beijing, 100049

3 Chinese Academy of Meteorological ScienCes, Beijing, 100081

Abstract

A three-dimensional hail-bin cloud model coupled with electrification process has been developed and used for simulating electrical charging and lightning processes in a severe thunderstorm in Beijing City in China. The results indicate that:1) The charge transfer between cloud droplets and graupel, and spatial distribution of charge density are primarily influenced by cloud water through inductive charging mechanism. However, when including rain water content the non-inductive charging between graupel and snow (or ice) crystals in different liquid water content may have important influences on the distribution of charge density through influencing the polarity and quantity of charges. 2) Different microphysical processes may produce the inhomogeneous distribution of the source and sink of hydrometeors. It causes the inhomogeneous distribution of hydrometeors in different vertical cross sections and leads to the complicated charge separation due to both inductive and non-inductive charging processes. At the same time, the charge transfer due to mass transfer of hydrometeors is not homogeneous.3) Ice phase hydrometeors are carried to higher altitude by strong updraft and transfer charges there. There are several centers of snow crystal content on the top of and on flanks of strong updraft , while graupel distribute relatively homogeneously , centers of content inclining to windward side of updraft. Therefore, non-inductive charging process mainly occurs at the windward side of updraft where divergence of air flow occurs, which cause the total charge density to distribute at the area. Due to strong updraft, several content centers of ice phase hydrometeors form in different areas and one category of hydrometeor may carry charge with different polarity (or quantity) in different areas, especially in the mature stage of severe thunderstorm, so that the multi-layer structure of charge is easy to develop.
4) Discharge changes electric structure. Induced charges at lightning channels are redistributed to each

hydrometeor category. And then, microphysical and dynamical processes complicate the charge transfer in the process of the mass transfer of hydrometeors, then the electric structure. Further research on the importance of lightning to electric structure is needed.

All the factors mentioned above play important roles in producing the multi-layer distribution of electric charges.

Key words: three-dimensional hail-bin cloud model, liquid water content, microphysical process, dynamical process, lightning flash

1 Induction

Electrification and discharge processes of severe thunderstorms are closely relevant to the development and evolution of cloud dynamical and microphysical processes. The field observations of cloud electrification and discharge processes are still difficult today. Laboratory study and numerical model are two important ways to study electrification mechanisms of thunderstorms. With the development of electrification theories, the ion capture process is not the emphasis any more for the study on numerical simulation. Researchers begin to consider more factors in models for the separation of charge and the corresponding microphysical processes. *Ziv and Levin* [1974] simulated the growth of the electric field in thunderclouds by polarization mechanism in a time-dependent numerical model. *Scott and Levin* [1975] investigated the growth of precipitation, the formation of electrical charges on the particles, and the development of the ambient electric field utilizing the polarization charging mechanism.

From the late 1970's, more numerical simulations on electrification put the emphasis on cold cloud processes. *Takahashi* [1978] found appreciable charges separated caused by collision between graupel and ice crystals. *Jayarantne et al.* [1983] got a different result. However, *Sanuders's* [1998] results were similar to *Takahashi's*. *Takahashi et al* [2002] himself reexamined his conclusions and found no differences.

Based on laboratory studies, researchers coupled the inductive charging (InC) and the noninductive charging (NInC) processes with cloud models to investigate characteristics of microphysics, dynamics and electrification inside thunderstorms. Results of models [e.g., *Chiu.*, 1978; *Rawlins.*, 1981; *Takahashi.*, 1984; *Helsdon and Farley.*, 1987; *Ziegler.*, 1989; *Yan.*, 1996; *Sun.*, 2002; *Mansell.*, 2005] showed that InC and NInC processes were predominant in the process of the separation of charges. Except dipole and tripole charge structures, overlapped charge structures more than four layers [*Stolzenburg.*, 1996] and the opposite polarity charge structures [*Krehbiel et al.*, 1999] have been observed too. Furthermore, charges with different polarities might exist at the same altitude [*Guo*, 2003].

Laboratory studies [e.g., *Takahashi.*, 1978; *Jayarantne et al.*, 1983; *Saunders et al.*.,1991] have confirmed that liquid water content (LWC) has a important influence on electrification and that the polarity of charge separated from hydrometeors lies on temperature and LWC together in the NInC process. However, the development of microphysical processes would influence distribution of LWC notably. Thus, microphysical processes play very important roles on electrification in thunderstorms too. It is still unclear how microphysical processes influence electrification and how discharge influences the distribution of charge density in thunderstorms.

In this paper, a three-dimensional hail-bin cloud model coupled with electrification has been developed and used for electrical charging and lightning processes in a severe thunderstorm on 23th, in August 2001 in Beijing City in China [*Fu.*,2003]. Influences of LWC, dynamical processes, microphysical processes and discharge on charge structures are investigated.

2 Model description

The numerical model in the present study is based on the hail-bin cloud model developed by *Guo and Huang* [2002]. Electrification and discharge processes are coupled with the model.

Only the InC process between cloud droplet and graupel and the NInC process between ice crystals (and snow crystals) and graupel are included in the model. The InC scheme is adapted from *Chiu* [1978] and the NInC scheme is adapted from *Takahashi* [1978]. Separated charges by mass transfer (not include microphysical processes involving vapor) are included in the sink and source of charge densities of hydrometeors and the separated charge is in proportion to hydrometeors' total area as a result of the mass transfer.

There are few quantitative results available on charge separation at temperature less than -30$^{\circ}C$ and the charge separation at low temperature may be less. In our model, all cloud droplets are homogeneously frozen at temperatures less than -40$^{\circ}C$. And we limit separated charges at temperatures less than -30$^{\circ}C$ by an arbitrary factor β [*Mansell.*, 2005]:

$$\beta = \begin{cases} 1 & : \ \mathrm{T} > -30^{\circ}\mathrm{C} \\ 1 - \left[1 - (\mathrm{T}+30)/10\right] & : \ -40^{\circ}\mathrm{C} < \mathrm{T} < -30^{\circ}\mathrm{C} \\ 0 & : \ \mathrm{T} < -40^{\circ}\mathrm{C} \end{cases}$$

According the result of *Marshall et al.* [1995], initiation threshold of lightning is

$E_{be} = \pm 167\,\rho(z)$

where E_{be} has units of kilovolts per meter, and z is the altitude（in kilometers）, and $\rho(z)$ is the air density (in kilometers per cubic meter）. Other schemes about the conduction of lightning are the same as *Mansell* [2002].

Simulations are integrated to 4800 s using a horizontal grid spacing of 1 km over a 36×36 km domain and a vertical grid spacing of 0.5 km over 19 km depth. Temperature and water vapor impulses with maximum excesses of 1.5 K placed in the center of the model domain with a size of 8×8 km in the horizontal and 2 km altitude (AGL) in the vertical is used to initiate convection in a horizontally homogeneous environment

3 Result

Figure1 shows charge density and temperature at different vertical cross sections at different time. ‘max’ and ‘min’ represent the maximize and minimum values at certain vertical cross section respectively.

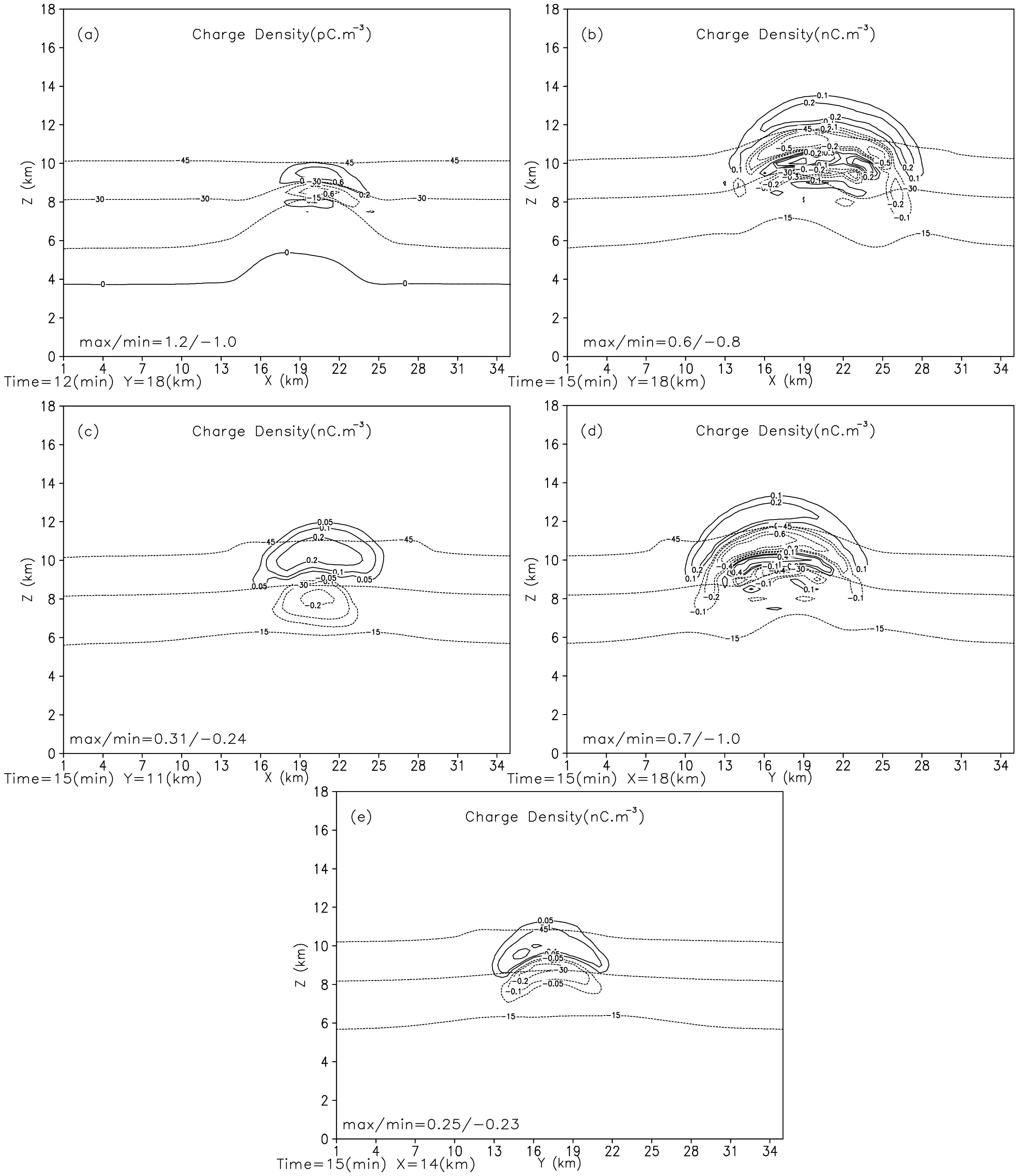

Fig.1 The vertical cross sections of the charge density (unit: nC/m^3 or pc/m^3, contour) and temperature (unit: ℃, horizontal contour). (a) t = 12 min and y = 18 km,(b)t = 15 min and y = 18 km, (c)t = 15 min and y = 13 km, (d)t = 15 min and x = 18 km, (e)t = 15 min and x = 14 km. Contours of charge density in (a) are ±0.2 and ±0.6 pc/m^3, in (b) and (e) are ±0.1, ±0.2 and ±0.5 nC/m^3, in (c) are ±0.05, ±0.1 and ±0.2 nC/m^3, in (d) are ±0.1, ±0.2 and ±0.6 nC/m^3. The contours interval of temperature is 15℃. Solid is for positive and dotted is for negative.

At t = 11 min, graupel has formed and electrified quickly. At t = 12 min , the distribution of the total charge density inside the cloud shows a weak positive tripole structure（Figure 1a） at y = 18 km cross section at 8 to 11 km altitude (-45℃ ≤ T ≤ -11℃).

The maximum charge density of the upper positive region caused by positively charged ice and snow crystals, is about 1.2 pC m^{-3} near z = 9.5 km altitude. And the minimum charge density of the middle negative region due to negatively charged graupel and snow crystals brought to above the reversal level by updraft after colliding with graupel is -1.0 pC m^{-3}. The lower positive region due to positively charged graupel brought to above the reversal level by updraft is near z = 7.5 km altitude, with the maximum charge density of 0.5 pC m^{-3}. The region of the total charge density extends only 6 km horizontally and the order of the charge density is small because the content of hydrometeors and the region where collision among hydrometeors occurs is not great.

At t = 15 min, the updraft reachs its maximum value. At the vertical cross section of y = 18 km, distribution of the charge density shows an arrangement of five-layer alternation of positive and negative region at z = 7.5 to 13 km altitude (-60℃ ≤ T ≤ -18℃) (Figure 1b). Furthermore, there exist charges with different polarities in different regions at the same altitude. Then, nearly each hydrometeor category carries charges with different polarities in different regions. The maximum net positive charge density (EtpMax) and minimum net negative charge density (EtpMin) are 0.6 nC m^{-3} and -0.8 nC m^{-3} respectively. The upper positive region is still mainly caused by snow crystals and ice crystals. While middle and lower charge region are mainly caused by graupel. For cloud droplets and rain droplets, their charge densities are less than ones of snow crystals and graupel. And they influence the electric structure only in local regions of the thundestorm.

At the vertical cross section of y = 11 km, the arrangement of the total charge density is a regular positive dipole (Figure 1c). The net positive charge region is still mainly caused by snow crystals and ice crystals. Now cloud and rain droplets charge positively and contribute less to the total charge density. The lower net negative charge region is mainly caused by graupel. At z = 10 and z = 8 km altitude, EtpMax and EtpMin are 0.31 nC m^{-3} and -0.24 nC m^{-3} respectively.

The distribution of charge densities at z-x vertical cross sections is similar to the one at z-y cross sections. At x = 18 km cross section, the electric structure shows a multi-layer distribution (Figure 1d), while at x = 14 km cross section, it shows a regular positive dipole structure (Figure 1e).

From the above, it is notably different for the distribution of charge density in different vertical cross sections or in different regions of the same vertical cross section. Four possible reasons will be discussed:

3.1 Influence of LWC on electric structure

LWC is one of the most important factors influencing electrification. Most results from laboratories [e.g., *Zhang and Liu*, 1999; *Pereyra et al.,* 2000] indicate that graupel charges positively at higher temperature or low LWC, otherwise charges negatively. The direct influence on electrification from the LWC will be discussed firstly.

As one part of LWC, CWC influences electric structures of the thunderstorm mainly through the InC process (another influence see 3.2). Figure 2a and Figure 2b show regions of collision between graupel and cloud droplets at different vertical cross sections at t = 15 min.

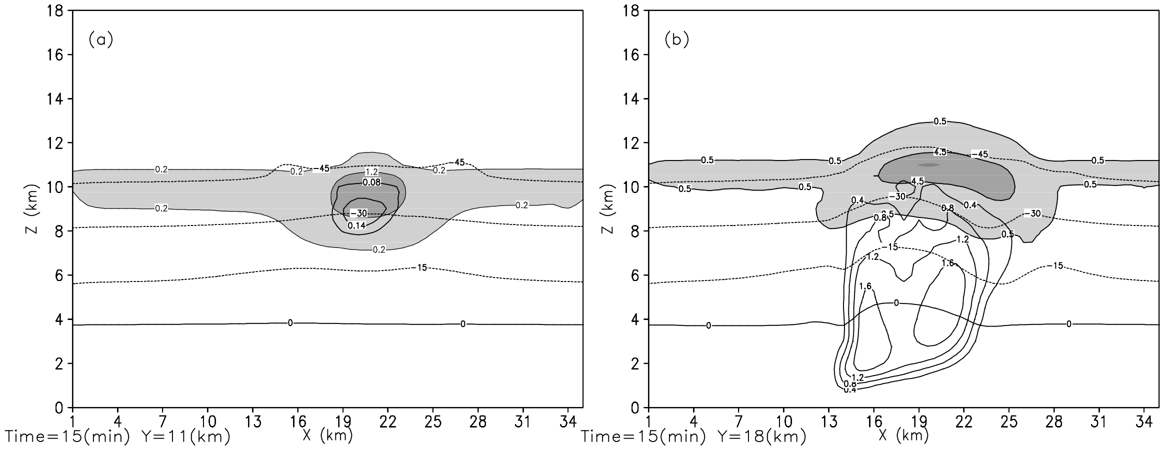

Fig.2 The x-z vertical cross sections of the water content(unit: g/m^3) of graupel(shaded area) and cloud water(solid line) and temperature(horizontal contour, unit:℃) at t = 15 min: (a)y = 11 km. The graupel content of light shaded is greater than 0.2 g/m^3, and of dark shaded is greater than 1.2 g/m^3.The contour interval of cloud water is 0.06 g/m^3. (b)The graupel content of light shaded is greater than 0.5 g/m^3, and of dark shaded is greater than 4.5 g/m^3.The contour interval of cloud water is 0.4 g/m^3. The contour interval of temperature is 15℃. Solid is for positive and dotted is for negative

Figure 3a and Figure 3b show densities of separated charges between graupel and cloud droplets due to the InC process at different vertical cross sections at t = 15 min.

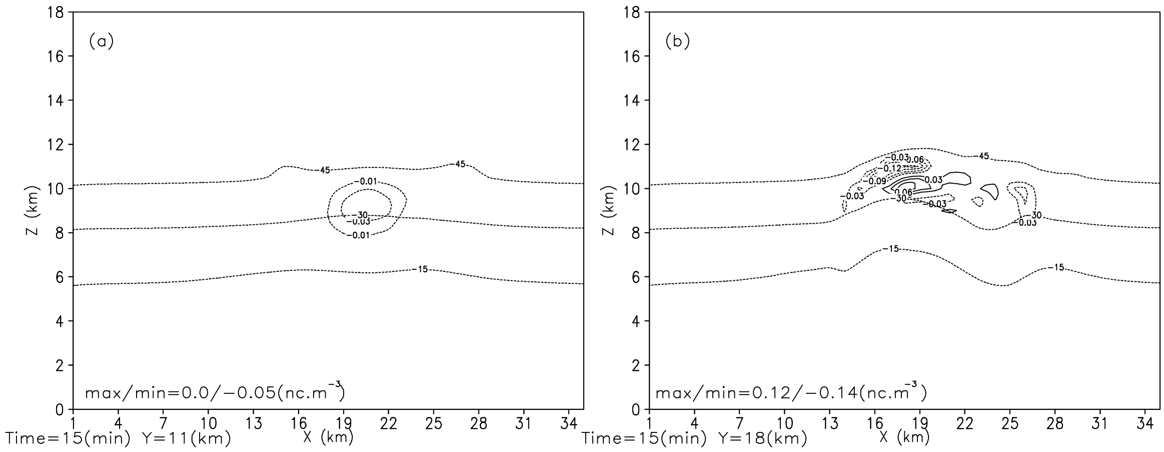

Figure 3 The x-z vertical cross sections of charge density (contour, unit: nC m^{-3}) transfer as a result of inductive-charging between graupel and cloud water and temperature(horizontal contour, unit: ℃).The contour interval of charge density in (a) is 0.02 nC m^{-3}, in (b) is 0.03 nC m^{-3}. The contour interval of temperature is 15℃. solid is for positive and dotted is for negative.

The homogeneous distribution of cloud droplets and graupel at collision region

(Figure 2a) result in the homogeneous distribution of the density of separated charges (Figure 3a) caused by the InC process at y = 11 km cross section. However, at y = 18 km cross section, the density of separated charges caused by the InC process (Figure 2b) fluctuates as a result of fluctuation of cloud droplets content in collision region (-40℃ ≤ T ≤ -25℃) (Figure 3b). Comparing to y = 11 km cross section where graupel only chargeds negatively by the InC process, graupel gains charges with different polarities and orders in different regions at y = 18 km cross section where there are several net negative charge regions around the net positive charge region. Graupel distributes relatively homogeneously, then, the fluctuations of the cloud water complicates the polarity of separated charge by InC process.

Through this way, the distribution of cloud water in different vertical cross sections influences the InC process, then the electric structure finally.

The electric structure and electrification processes at the vertical cross section of y = 18 km at t = 12 min are similar to ones at y = 11 km cross section at t =15 min.

Influence of LWC including rain water on electric structure will be discussed.

Due to the strong updraft and other microphysical processes, most of ice crystals climb over the -40℃ level when graupel starts to develop. Therefore, the NInC process between graupel and snow crystals influencs electric structure more.

Takahashi [1978] pointed out graupel charged positively in the NInC process when LWC was ranged from 0.1 to 4.0 g m^{-3}, otherwise charged negatively above the reversal level and negatively below the reversal level. According the analysis in 3.1, LWC of the case is substantial. At t = 14.5 min, the region where LWC is greater than 4.0 g m^{-3} in some vertical cross sections (such as at y = 18 km) has formed above the reversal level (Figure 3a). Graupel charges positively where LWC is less than 0.1 g m^{-3} or greater than 4.0 g m^{-3} (Figure 3b).

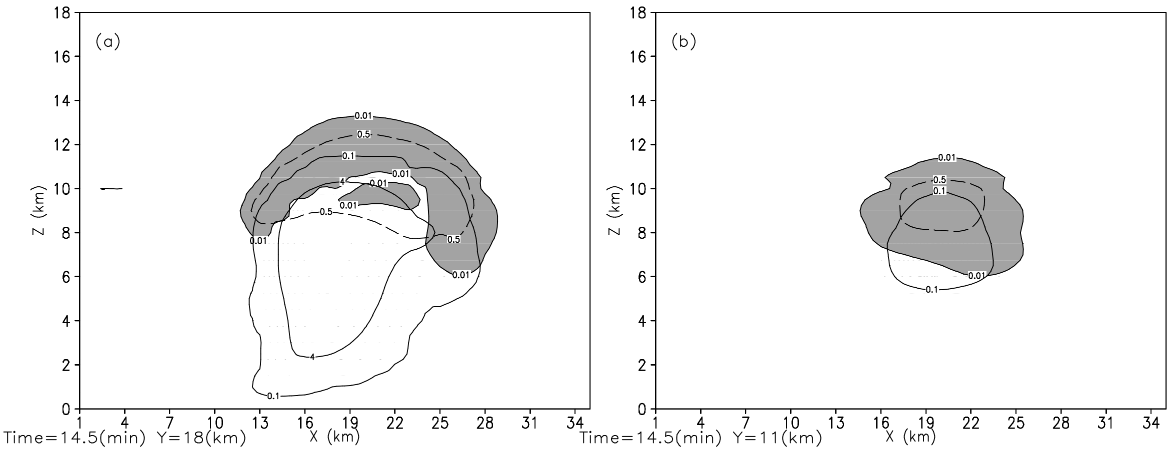

Fig. 4 The x-z vertical cross sections of the water content (unit: g m^{3}) of liquid (solid line), graupel (long dotted line) and snow crystal(shaded area). Water content in shaded area is greater than 0.01 g m^{3}. Long dotted line is 0.5 g m^{3}. Solid lines in (a) are 0.1 g m^{3}, 4.0 g m^{3} respectively and solid line in (b) is 0.1 g m^{3}

At some vertical cross sections (such as y = 11 km), LWC above reversal level is less than 4.0 g m^{-3}. Therefore, only in collision regions where LWC is less than 0.1 g m^{-3} (Figure 4a), could graupel gain positive charge (Figure 4b) by the NInC process.

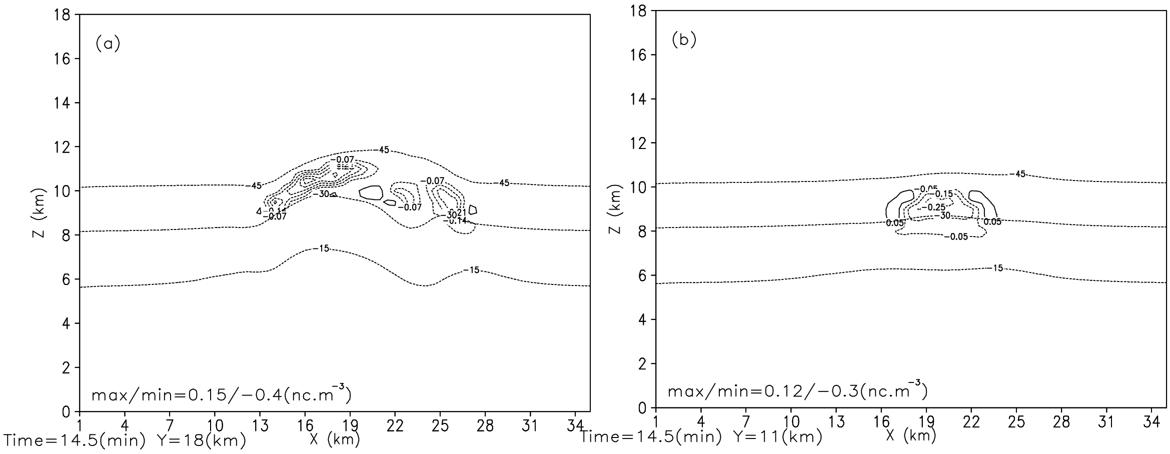

Fig.5 The x-z vertical cross sections of the charge density(contour, unit: nC/m^3)transfer as a result of non-inductive charging between graupel and snow crystal and temperature(unit: ℃, horizontal contour) at t = 14.5 min. The contour interval of charge density in (a) is 0.07, in (b) is 0.1 nC m^{-3}. The contour interval of temperature is 15℃. Solid is for positive and dotted is for negative.

Note that charge separation by the NInC process reduces rapidly when LWC is less than 0.1 g m^{-3} in Takahashi's scheme. Accordingly, the distribution of electric structure depends more on the region where LWC is greater than 0.1 g m^{-3}. As mentioned above, in our simulation, charges of graupel and snow crystals are mainly from the NInC process. The substantial supercooled water complicates the distribution of separated charges in polarity and quantity.

Therefore, cloud water influences the total charge density mainly through the InC process between cloud droplets and graupel. While liquid water including rain water influences the total charge density mainly through the NInC process between graupel and snow (or ice) crystals.

3.2 Influences of microphysical process on electric structures

Strictly, microphysical process acts together with dynamical and electrical processes together. For the convenience of discussing the direct influence of microphysical processes on electric structures, we will investigate the influence through two ways: 1) by influencing the distribution of hydrometeors to influence electric structure; 2) by influencing the mass transfer among hydrometeors to influence electric structure.

As mentioned in 3.1, fluctuation of the cloud water complicates charge transfer between graupel and cloud droplets. However, comparing to the InC process, the NInC process has more important influence on electric structures [e.g., *Chiu.*, 1978; *Takahashi*, 1978, 1984; *Helsdon et al.*, 1987; *Ziegler et al.*, 1989; *Mansell et al.*, 2005]. In this case, the NinC process between graupel and snow crystals is the predominant factor influencing electric structure because most of ice crystals are above -40℃ level when graupel begins to develop.

Hydrometeors experience complicated microphysical processes when developing. Predominant factors influencing the development of hydrometeors are always not same in different vertical cross sections. In our model, collision between cloud water and snow crystals and the freezing of supercooled water are two important factors to the development of snow crystal. ACLcs and ANUrs represent the increase of the content of snow crystals (Qs) due to the two factors mentioned above respectively.

The distribution of Qs and increase of Qs caused by ACLcs and ANUrs at different vertical cross sections at t = 14.5 min is shown in Figure 5.

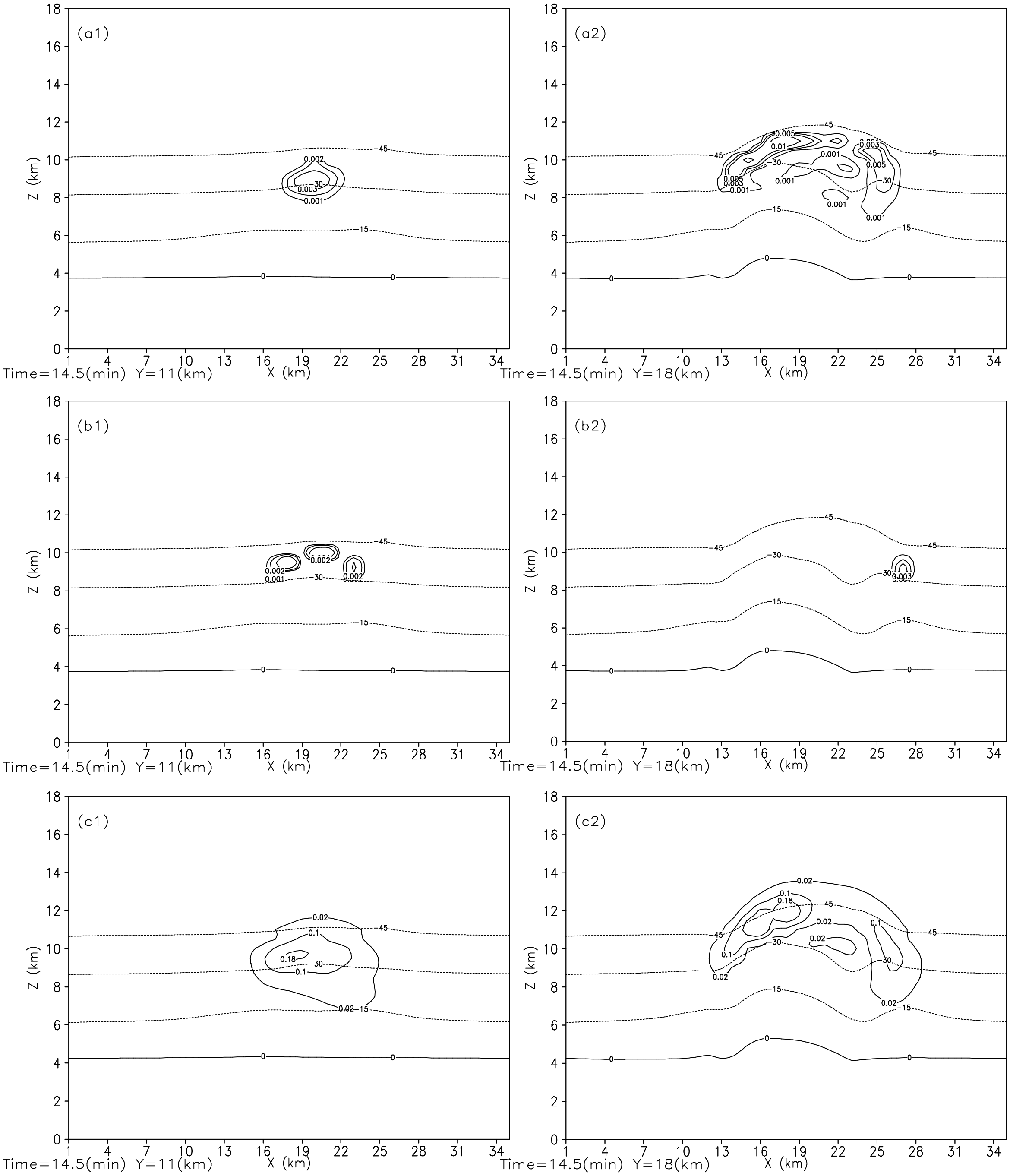

Figure 6 The x-z vertical cross sections of the water content increase (solid line, unit:g m^{-3}) of snow

crystal as a result of the collision between snow crystal and cloud water(a1,a2), the freezing of supercooled raindrops (b1,b2) and the water content (solid line, unit: g m^{-3},c1,c2) of snow crystal and temperature(horizontal contour, solid is for positive, dotted is for negative, unit: ℃). Contour intervals in (a1),(a2),(b1),(b2),(c1),(c2) are 1×10^{-3} g m^{-3}, 2×10^{-3} g m^{-3}, 1×10^{-3} g m^{-3}, 2×10^{-3} g m^{-3}, 0.06 g m^{-3}, 0.06 g m^{-3} respectively. The contour interval of temperature is 15℃.

The distribution of ACLcs is homogeneous in Figure 5a1. Comparing to the maximum Qs, 0.18 g m^{-3} (Figure 5c1), ACLcs, with the maximum value of 0.005 g m^{-3}, contributes less to the increase of Qs. While ACLcs in the cross section of y = 18 km distributes non-homogeneously and there are several water content centers with the maximum value of 0.02 g m^{-3} (Figure 5a2). The maximum Qs in the section is 0.35 g m^{-3} and the center of Qs is nearly consistent with the center of ACLcs (Figure 5c2). Therefore, ACLcs at y = 18 km cross section contributes more to the increase of snow crystals comparing to ANUrs.

Figure 5b1 and 5b2 show the increase of Qs caused by ANUrs at cross sections of y = 11 km and y = 18 km respectively at t = 14.5 min. At y = 11 km cross section, the center of ANUrs is near x = 17.5 km, with the maximum value of 0.01 g m^{-3}. The other two centers of ANUrs contribute less to Qs for less orders. Centers of ANUrs are consistent with ones of Qs. However, the order of ACLcs is small and ACLcs contributes less to Qs. At y = 18 km cross section, comparing to the maximum Qs of 0.35g m^{-3}, the maximum ACLcs is only 0.007g m^{-3}. It contributes to the increase of Qs only at local regions of the thunderstorm. Therefore, ANUrs at y = 11 km cross section contributes more to the increase of snow crystals comparing to ACLcs.

From the analysis above, the non-homogeneousness of predominant factors to accretion of Qs make the distribution of Qs not homogeneous due to microphysical processes in different vertical cross sections, which enhances the non-homogeneousness of Qs. Of course, other influence factors such as consummation of snow crystals would result in the non-homogeneousness of Qs too. There are similar distribution and development processes for other hydrometeor categories. Detailed analysis is neglect.

The non-homogeneous distribution of hydrometeors caused by microphysical processes make InC and NInC processes (see 3.1) not homogeneous in different vertical cross sections. There are several centers of Qs and regions where collision between snow crystals and graupel occurs are not homogeneous at y = 18 km cross section in Figure 3a. Therefore, separated charges from the NInC process between snow crystals and graupel shows a complicated distribution in Figure 4a. While it is not so at y = 18 km cross section in Figure 4b as a result of the homogeneous distribution of Qs and Qg (content of graupel) (Figure 3b). Causes of the non-homogeneousness of polarity of separated charge by the InC process has been discussed, see 3.1 in detail.

The non-homogeneousness of microphysical processes in different regions results in the non-homogeneousness of the NInC process. And the non-homogeneousness of mass transfer of hydrometeors results in the non-homogeneousness of charge transfer.

Figure 6 shows charge transfer due to mass transfer of hydrometeors (CMC, CMR, CMI, CMS, CMG represent density of the gained charge by mass transfer of cloud droplets, rain droplets, ice crystals, snow crystals and graupel respectively, unit: nC/m^3) at y = 18 km cross section at t = 14.5 min.

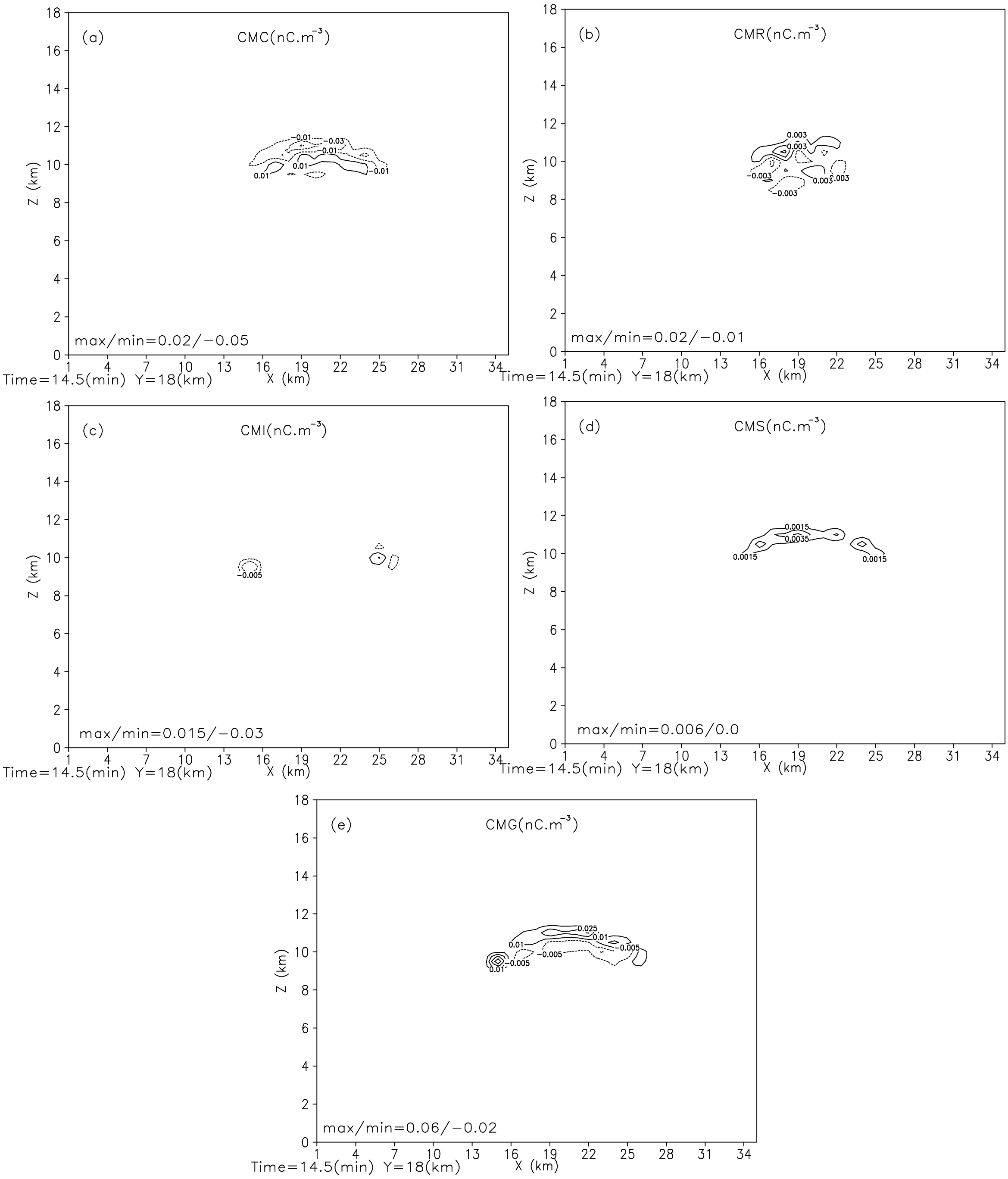

Fig.7 Figure 8 The x-z vertical cross sections of the sum of source and sink of the charge density (unit: nC m^{-3}) as the result of the mass transfer of hydrometeors.(a) cloud water, (b) rain water, (c) ice crystal, (d) snow crystal, (e) graupel. Contour intervals from (a) to (e) are 0.02, 0.006, 0.01, 0.002, 0.015 nC m^{-3} respectively. Solid is for positive and dotted is for negative.

At this time, the maximum and minimum charge densities of cloud droplets (Qec) are

0.12 nC m^{-3} and -0.04 nC m^{-3} respectively. There are several charge centers with different polarities in CMC (Figure 6a) and the maximum and minimum value are 0.02 nC m^{-3} and -0.05 nC m^{-3} respectively. While the charge of cloud droplets gained from the InC process contributes a little more to Qec, with the maximum and minimum value are 0.16 nC m^{-3} and -0.06 nC m^{-3} respectively.

The maximum and the minimum CMR are 0.02nC m^{-3} and -0.01nC m^{-3} respectively in Figure 6b. And the maximum and minimum charge densities of rain droplets (Qer) are 0.03 nC m^{-3} and -0.03 nC m^{-3}. Before snow crystals and graupel begin to melt, the main charge source of rain droplets is cloud droplet. Therefore, non-homogeneous distribution of Qec makes rain droplets gain charges with different polarities in different regions. That is to say, whether the distribution of Qer is homogeneous or not mainly depends on the distribution of Qec before melting of snow crystals and graupel. It's just the second kind of influence of cloud droplets on total charge density mentioned in 3.1.

The positive region of CMI is a little far from the negative region in Figure 5c, with the maximum and minimum vaule of 0.015 nC m^{-3} and -0.03 nC m^{-3} respectively. And the maximum and minimum charge densities of ice crystals (Qei) are 0.03 nC m^{-3} and -0.025 nC m^{-3} respectively. Due to the limited regions of collision with graupel, the distribution of Qei gained from the NInC process shows a single polarity structure with the maximum positive value of 4.5×10^{-3} nC m^{-3}, which contributes a little less than CMI to Qei as a result of the weaker charge separation by the NInC process for most of ice crystals climb over -40℃ level. However, the NInC process may contribute less in other vertical cross sections (detailed analysis is neglected). Generally, the two factors have the same important influences on Qei.

There is only one positive region in CMS with the maximum density of 6×10^{-3} nC m^{-3} in Figure 5d while the maximum and the minimum net charge densities of snow crystal (Qes) due to the NInC process are 0.35 nC m^{-3} and -0.1 nC m^{-3} respectively, and the maximum and the minimum Qes were 0.5 nC m^{-3} and -0.3 nC m^{-3} respectively.

The maximum and the minimum CMG are 0.06 nC m^{-3} and -0.02 nC m^{-3} respectively and the maximum and the minimum charge densities of graupel (Qeg) are 0.4 nC m^{-3} and -0.8 nC m^{-3} respectively in Figure 5e. Obviously, the order of CMG is less than Qeg gained from the NInC process.

Non-homogeneous distribution is one common characteristic of CMC, CMR, CMI, CMS and CMG.

For each hydrometeor category, the influence of charge transfer on charge density caused by mass transfer is very different. As for cloud droplets, rain droplets and ice crystals, the order of their charge densities is almost equivalent to the one of CMC, CMR and CMI respectively. Therefore, non-homogeneousness of CMC, CMR and CMI makes Qec, Qer and Qei more non-homogeneous in local regions of the thunderstorm. The order of CMS is a little less than Qse. Maybe it is caused by our model itself. The accretion of snow crystals mainly comes from cloud droplets, rain droplets and ice crystals in our model. However, the order of charge density of each of the particle mentioned above is less than the one of Qes and Qeg. Although the distribution of CMS is extensive, only in local regions where CMS is greater, could CMS contribute dramaticly to Qes. For the same reason, the order of CMG is not greater. However, it is a little greater than CMS, which maybe because Qse with greater order than the charge density of other hydrometeors except graupel affords charges to graupel when experiencing mass transfer through microphysical processes such as collision and auto conversion et al.

At y = 11 km cross section, microphysical process is relatively homogeneous, therefore, charge transfer caused by mass transfer is relatively homogeneous too. Detailed analysis is neglected.

In a word, the non-homogeneousness of microphysical process results in the non-homogeneousness of the sink and source of water content of hydrometeors in different vertical cross sections. And then, it results in the non-homogeneousness of the InC and NInC processes (especially for snow crystals and graupel) and of charge transfer caused by mass transfer, especially for rain droplets. As for cloud droplets and ice crystals, influences of two factors are nearly the same.

Although we discussed only at two different vertical cross sections at t = 14.5 min, it could represent two kind of different phenomena in the process of evolution of the thunderstorm.

According the analysis above, by direct influence of LWC and microphysical process, it's possible for hydrometeors (especially for snow crystals and graupel) to electrify with different polarities in different regions at certain time. When distribution of Qse and Qeg is non-homogeneous, electric structure may show the arrangement of three layers or more (such as the total charge density at y = 18 km cross section at t = 15 min). Other kind of hydrometeors would influence electric structure at certain local regions.

3.3 Influence of dynamical process on electric structure

In this section, influence of dynamical process on electric structure will be discussed from the point of updraft and environmental wind.

Figure 7 shows the vertical cross section of updraft (greater than 30 m/s), ice crystals and temperature at y = 18 km at t = 12 min. The thunderstorm is in initial development stage and sizes of ice crystals are a little small. The center of updraft is above -15℃ level and most of ice phase hydrometeors are carried to above -30℃ level. The separation of ice phase hydrometeors due to the updraft is not dramatic. Therefore, charge distributes mainly above -15℃ level at the cross section of y = 18 km in Figure 1a.

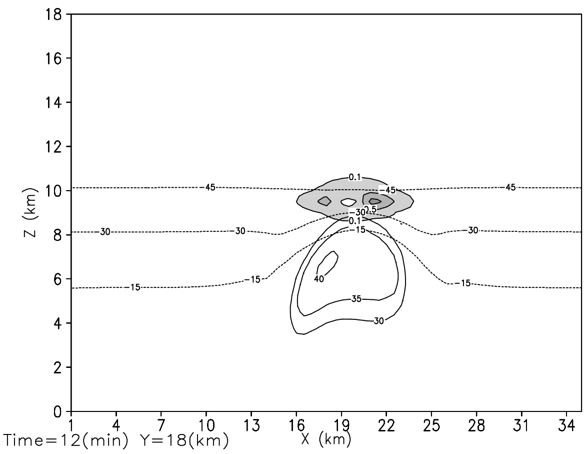

Fig.8 The x-z vertical cross section of vertical updraft (unit: m/s, contour, greater than 30 m s^{-1}, interval is 15 m s^{-1}), the ice phase hydrometeors (unit: g/m^3, shaded area, dark shaded is greater than 0.9 g m^{-3}) and temperature (unit: ℃, horizontal contour, interval is 15 ℃) at y = 18 km at t = 12 min.

Updraft is strengthened quickly with the development of the thunderstorm. As described in 3.2, ice crystals distributs mainly above -40℃ level in the evolution of the thunderstorm. Influence of updraft and environmental wind field to charge separation of snow crystals and graupel would be discussed in the following.

Figure 8 shows the vertical cross sections of Qg, Qs and wind vector field at y = 18 km and y = 11 km at t = 15 min.

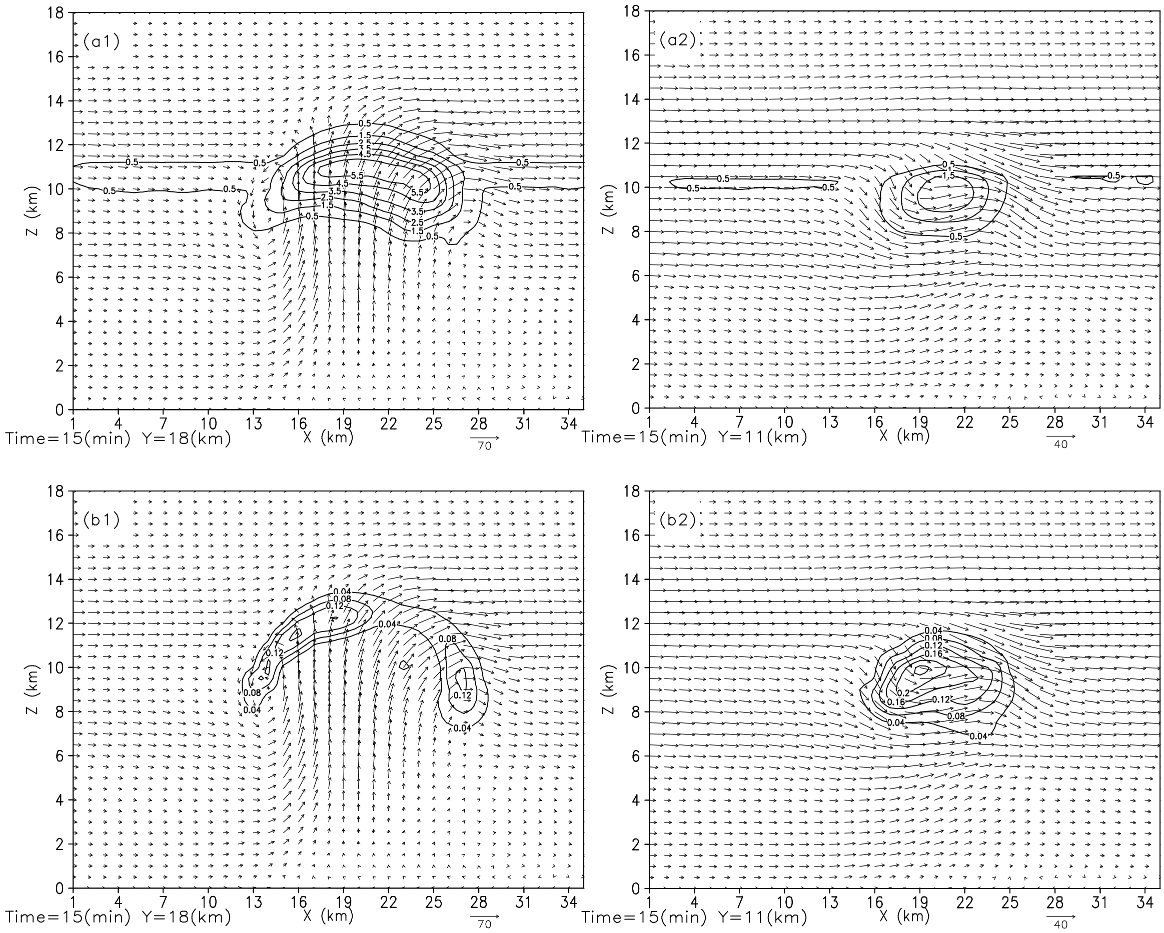

Fig.8 The x-z vertical cross sections of graupel content and snow crystal content (contour, unit: g m^{-3}) and wind vector field (arrow) at t = 15 min: (a1) y = 18 km, graupel, (a2) y = 11 km, graupel, (b1) y = 18 km, snow crystal, (b2) y = 11 km, snow crystal. The contour interval in (a1) and (a2) is 1.0 g m^{-3}, in (b1) and (b2) is 0.02 g m^{-3}.

At the vertical cross section of y = 18 km, though updraft is very strong, graupel still distributes homogeneously and mainly positions at upper part of the updraft (Figure 7) for the greater sizes. Furthermore, the center of Qg inclines a little to the windward side of the updraft (Fig 8a1) (略向迎风侧倾斜) as a result of strong west wind field and divergence of air flow at higher altitude (高层强的西风场及辐散出流). However, snow crystals are influenced more by factors mentioned above for their less sizes. There are three centers of Qs at the upper part and two flanks（两侧） of the updraft (Figure 8b1). That is to say, snow crystals develop mainly at these areas. Therefore, the NInC process between snow crystals and graupel occurs not at centers of the strong updraft but at regions mentioned above where charge exchange processes between snow crystals and graupel occurs easily.

At the y = 11 km cross section, the updraft is weaker. The development of graupel and ice crystals is influenced mainly by environmental wind field. Therefore, Qg and Qs distributed more homogeneously (Figure 8a2 and Figure 8b2), which causes the NInC process between graupel and snow crystals more homogeneously.

Figure 9 shows the vertical cross sections of Qg, Qs and wind vector field at y = 18 km at t = 16.5 min when the first intra-cloud flash is initiated.

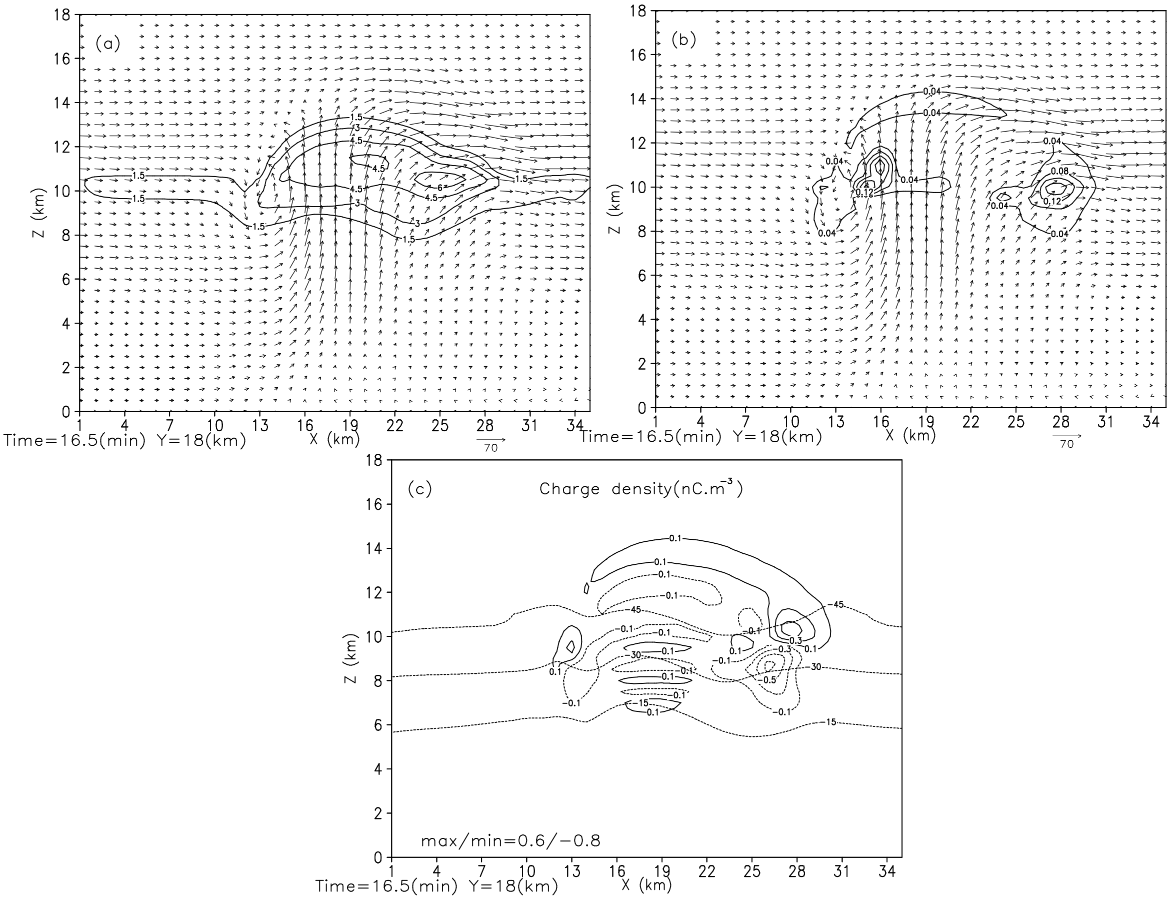

Fig.9 The x-z cross sections at y = 18 km of graupel content and snow crystal content (contour， unit: g/m^3), wind vector field (arrow) ,charge density (contour, unit: nC/m^3, solid is for positive and dotted is for negative) and temperature (horizontal contour, unit: ℃) at t = 16.5 min : (a) graupel content and wind vector field, (b) snow crystal content and wind vector field, (c) charge density and temperature. The contour interval in (a) is 1.5 $g\ m^{-3}$, in (b) is 0.04 $g\ m^{-3}$, in (c) is 0.2 $nc\ m^{-3}$.

Influenced by environmental wind field and air flow's divergence (辐散气流) , the center of Qg inclines to the windward side of the updraft (偏向迎风侧) dramaticly (Figure 9a), while there are three centers of Qs at the upper part and two flanks (两侧) of the updraft. The collision area of graupel and snow crystals inclines to the windward side of the updraft (向迎风侧倾斜), therefore, the center of charge density does so.

From the analysis above, ice phase hydrometeors are carried to higher altitude, therefore, charge separation occurs at higher altitude. There are several centers of Qs at the upper part and two flanks of the strong updraft. While graupel distributes relatively homogeneous and centers of Qg inclines to the windward side of the updraft. Therefore, the NInC process occurs mainly at the windward side of the updraft where divergence of air flow occurs (上升气流迎风侧的辐散区域) and separates charges distributed there. Therefore, the strong updraft and environmental wind causes ice phase hydrometeors form several centers at different areas and causes certain ice phase hydrometeor carry charges with different polarity at different areas (especially at the mature stage of the thunderstorm, detailed analysis neglected). Therefore, they make it easy for charge density to produce multi-layer structure.

It's similar at vertical cross section x = 18 km and x = 14 km.

3.4 Influence of lightning flash on electric structures

The updraft begins to fallback and the first intra-cloud (IC) flash initiated at t = 16.5 min.

Figure 10 shows the density and leaders at different vertical cross sections. Note that lightning channels at vertical cross sections are not projections but paths of leaders in corresponding vertical cross sections.

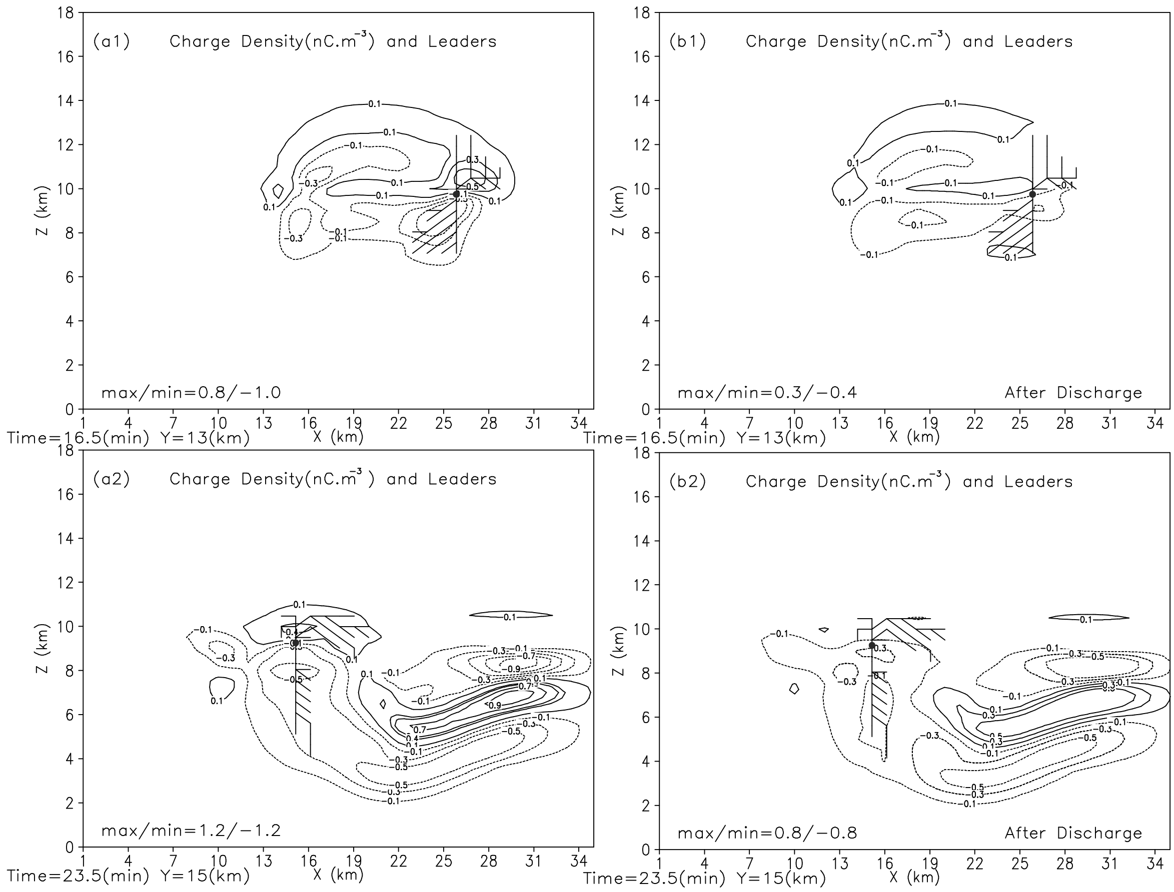

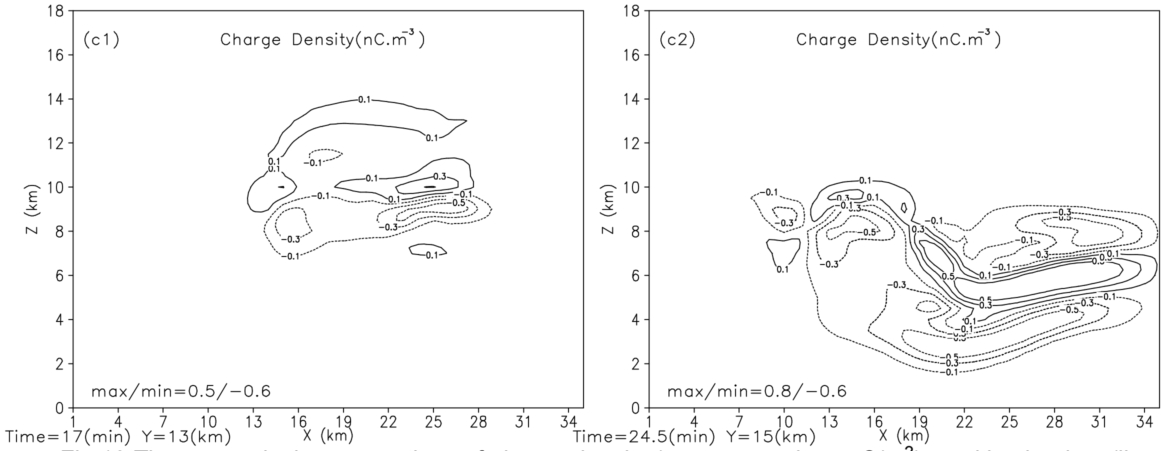

Fig.10 The x-z vertical cross sections of charge density (contours, unit： nC/m^3), positive leaders (lines downward from the black solid circle) and negative leaders (lines upward from the black solid circle) at different time: (a1)t = 16.5 min, y = 13 km, pre-discharge, (b1)t = 16.5 min, y = 13 km, post-discharge, (c1)t = 17 min, y = 13 km, (a2)t = 23.5 min, y = 15 km, pre-discharge, (b2)t = 23.5 min, y = 15 km, post-discharge, (c2)t = 24.5 min, y = 15 km. The contour interval of charge density in (a1), (a2), (b1), (b2), (c1), (c2) is 0.2 nC m^{-3}.

Lightning flash initiates at the vertical cross section of y = 13 km at t = 16.5 (Figure 10a1). After initiation at x = 26 km that is the boundary of positive and negative regions, positive (negative) leaders propagated to the negative (positive) region from initiation point. Furthermore, positive (negative) leaders propagate through the center of negative (positive) charge region. This conclusion is consistent with the discharge model given by *MacGorman et al.* [2001] and some observations [e.g., *Shao and Krehbiel.*, 1996; *Coleman et al.*, 2003]. At the same time, greater changes occurs near and at channel grids (Figure 10b1), especially at the end of positive leader, where polarity of induced charges reversed. It is similar with some researchers' conclusions [e.g., *Mansell et al.*, 2005; *Tan and Zhu* et al., 2007]. *Coleman et al.* [2003] ever observed that opposite polarity charges deposited at lightning channels.

30 s later, charge density at and near channel grids resumes original distribution by and large (Figure 10c1).

Figure 10a2 shows the vertical cross section of lightning channels and charge density at y = 15 km at t =23.5 min. The updraft gets weaker and ice phase hydrometeors continue developing, therefore, ice phase hydrometeors (especially for graupel) descend to lower altitude. Caused by dynamical, microphysical and other processes, there are two centers of Qs formed at two flanks of the updraft and two centers of Qg developing near windward side of the. Therefore, several centers of charge density develop at this cross section. After initiation at x = 15 km that is the boundary of positive and negative regions, positive (negative) leaders propagate to the negative (positive) area from initiation point and positive (negative) leaders propagated through the center of negative (positive) charge area, which is similar to lightning channels at t = 16.5 min. The charge near and at channel grids changes, however, there are no charges with opposite polarity left at channels (figure 10b2). At t = 16.5 min, lightning flash initiates between main positive charge area and main negative charge area, furthermore, charge densities at lightning channels are greater. However, at t = 23.5 min, lightning flash originates between subpositive charge area and sub-negative charge area, and there exist several charge regions with greater densities at the windward side of the initiation point of flash (在闪电触发区顺风侧) at lower altitude. Although charge densities at channels are less than ones at lower altitude, electric fields at these areas have reached initiation thresholds. Therefore, lightning flashes initiate and propagate at areas with less charge density. 1 min later, charge densities at and near channel grids resume original positive dipole structures (figure 10c2).

From the analysis above, lightning flash influences the distribution of charge density no matter whether charges with opposite polarity were left at channels or not. Each hydrometeor category in lightning channels receives charge in proportion to its total surface area regardless of preexisting charges [*Mansell et al.*, 2002]. The more the channel segments, the more hydrometeors participating with redistribution of charges with opposite sign. According the analysis 4.2, hydrometeors carrying positive (negative) charge in mass transfer may carry negative (positive) charge after discharge and orders of charge, which depends on charges induced at channel grids, may be very different due to microphysical process. Therefore, discharge will complicate the distribution of the total charge density, and then complicate the charge density of each hydrometeor category at a relatively short time span.

4 Discussions

1) As we all know, graupel is the key factor to electrify. In our hail-bin cloud model, the real velocity of graupel is adapted. That is to say, graupel with different category falls at different velocity, which will make it easy for graupel to develop and distribute non-homogeneously. In our model, graupel with 21 categories will transfer charge with other hydrometeors respectively. Therefore, the InC and NInC processes are not homogeneously so that multi-layer of electric structure is produced easily. When weighed average velocity is adapted in microphysical scheme [e.g., *Sun et al.*, 2002], the accretion and distribution of graupel will be more homogeneous, which will cause the InC and NInC processes a little more homogenous. Thus, the total charge density will distribute more homogenously.

2）Schemes of electrification have important influences on discharge and characteristics of the charge density of each hydrometeor category. The efficiency of collision, the rebound probability, the average cosine of angle of rebounding collision, et al., which are always specified arbitrarily and influence the InC process very much [e.g., *Chiu.*, 1978; *Ziegler.*, 1989]. *Mansell* got different results with 5 different non-inductive charging schemes respectively in his model. Except due to the thunderstorm case itself, different schemes about microphysical processes in different models would influence the charge separation too. With a two-dimensional time-dependant and electric model, *Zhang and Liu* [1999] concluded that lightning flashes initiated mainly at t = 30 to 45 minutes after thunderstorms initiated when the maximum updraft became weaker. However, in this paper, the first IC flash initiated at t = 16.5 min (1.5 minutes after the maximum updraft got weaker). As far as the same case is concerned, different electrification schemes would result in different results. Further laboratory studies and more field observations are needed to verify the reliability of schemes.

3）In the total process of simulation, most ice crystals are mainly above the -40℃ level as a result of microphysical processes and the strong updraft together. Therefore, collision between graupel and snow crystals becomes the main source of the NInC process and the order of separated charges is greater than the one due to the InC process between graupel and cloud droplets.

4）There exist controversies in the influence of LWC on the reversal temperature [e.g., *Gardiner et al.*, 1985; *Pereyra et al.*, 2000; *Coleman et al.*, 2003], which has an important influence on electric structures of thunderstorms [*Guo.*, 2003]. Though the influence of LWC on the reversal temperature is not investigated in this paper, it would not interfere with discussing other influences of LWC, influences of microphysical and dynamical processes on electric structures of thunderstorms. The selection of charge scheme mainly influences the quantity and polarity of separated charge.

5) In this case, ice phase hydrometeors could be carried to higher level as a result of the strong updraft (Figure 2). Therefore, the NInC process occurred at higher level too, that is to say, ice phase hydrometeors separated charges at higher level (Figure 1). With the development of the thunderstorm, the updraft got weaker, ice phase hydrometeors descended (Figure1d, Figure 8c), therefore, charge density descended too (Figure 10a2, Figure 10b2).

6）Limited by the capability of computation, electric processes are coupled mainly in two-dimensional numerical models before. Although some simulated electric characteristics of thunderstorms in two-dimensional models are consistent with results of observations, it's not enough for investigating electric structures of three-dimensional space only in one vertical cross section due to the inhomogeneous distribution of the total charge density. After simulating a severe thunderstorm with a three-dimensional hail-bin cloud model in this paper, we find it very different for charge structures in different vertical cross sections. In different vertical cross sections, the charge structure may show a regular positive dipole or triple distribution, or show a very inhomogeneous distribution. It makes lightning flashes initiate in different vertical cross sections.

7） *Tan et al.* [2007] got approximate vertical lightning channels with less horizontal branches in a two-dimensional model with the resolution of 200 meters. However, channels got from our model with coarser resolution shows more horizontal branches. It might be caused by the propagation condition of leaders. *Tan* adapted a fixed value (150 kv/m) as the critical electric field. However, the critical electric field in this paper changed with the air density (or height) [e.g., *Marshall et al.*, 1995; *Mansell et al.*, 2002]. However, the critical electric field is less where the air density is less, which is consistent with observation [*Marshall et al.*, 1995]. Thus, more horizontal grids around channels are satisfied with conditions of propagation and it's easier for leaders to propagate horizontally. Results of simulation show opposite polarity charges deposited in channels, which is consistent with observations [*Coleman et al.*, 2003] and results of simulation [*Tan et al.*, 2007].

8) In our simulation, lightning left opposite polarity charge at channels sometimes, which is consistent with observation [e.g., *Coleman et al.*, 2003] and simulation results [e.g., *Mansell et al.*, 2005; *Tan et al.*, 2007]. However, it is not always so. Leaders just changed the distribution of charge densities on and near channel grids at t = 23.5 min. After lightning flash initiates, the time needed to resume the distribution of charge density (τ) on and near channel grids is different. At t = 16.5 min, τ is 30 s or so, while τ is 1 min or so at t = 23.5 min. τ is influenced by dynamical, microphysical and other processes, therefore, τ will change with model, resolution, scheme of flash neutrality et al. However, τ is sure to be much greater than the time of discharge.

9) The redistribution of charge after discharge is not ideal in our simulation. It's probably because of the simplified way to calculate induced charge on channels and the coarse resolution of our model. However, it is undoubted that lightning flash will influence the structure of total charge. Charge densities at lightning channel grids will change accordingly. And then, all the categories of hydrometeors at channel grids will receive charge which may be very different in polarity or order. Caused by dynamical and microphysical processes, induced charge in channels will complicate the distribution of total charge density. Therefore, the total charge density inclines to form centers in different areas so as to produce multi-layer structure. Observations about induced charge at lightning channels are still scarce and further research on influence of discharge on electric structures is needed.

5 Conclusions

A three-dimensional hail-bin cloud model coupled with electrification process has been developed and used for simulating electrical charging and lightning processes in a severe thunderstorm in Beijing City in China. The results indicate that:

1) The charge transfer between cloud droplets and graupel, and spatial distribution of charge density are primarily influenced by cloud water through inductive charging mechanism. However, when including rain water content the non-inductive charging between graupel and snow (or ice) crystals in different liquid water content may have important influences on the distribution of charge density through influencing the polarity and quantity of charges.

2) Different microphysical processes may produce the inhomogeneous distribution of the source and sink of hydrometeors. It causes the inhomogeneous distribution of hydrometeors in different vertical cross sections and leads to the complicated charge

separation due to both inductive and non-inductive charging processes. At the same time, the charge transfer due to mass transfer of hydrometeors is not homogeneous.

3) Ice phase hydrometeors are carried to higher altitude by strong updraft and transfer charges there. There are several centers of snow crystal content on the top of and on flanks of strong updraft , while graupel distribute relatively homogeneously , centers of content inclining to windward side of updraft. Therefore, non-inductive charging process mainly occurs at the windward side of updraft where divergence of air flow occurs, which cause the total charge density to distribute at the area. Due to strong updraft, several content centers of ice phase hydrometeors form in different areas and one category of hydrometeor may carry charge with different polarity (or quantity) in different areas, especially in the mature stage of severe thunderstorm, so that the multi-layer structure of charge is easy to develop.

4) Discharge changes electric structure. Induced charges at lightning channels are redistributed to each hydrometeor category. And then, microphysical and dynamical processes complicate the charge transfer in the process of the mass transfer of hydrometeors, then the electric structure. Further research on the importance of lightning to electric structure is needed.

All the factors mentioned above play important roles in producing the multi-layer distribution of electric charges.

References

Brooks,I.M.,C.P.R.Saunders,R.P.Mitzeva,and S.L.Peck (1997), The effect on thunderstorm charging of the rate of rime accretion by graupel, ,*Atmos. Res., 43*, 277-295.

Chiu C (1978), Numerical study of cloud electrification in an axisymmetric, time – dependent cloud model. *J. Geophys. Res., 83*, 5025-5049.

Coleman L M, Marshall T C , StolzenburgM, et al. (2003), Effects of charge and electrostatic potential on lightning propagation. *J . Geophys. Res .*, *108(D9)*, 4298, doi:10.1029/2002JD002718.

Fu Danhong, Guo Xueliang, Xiao Wenan, et al. (2003) Numerical study on the formation of a Severe storm accompanied with gale and heavy rain in Beijing, *Journal of Nanjing Institute of Meteorology*, *26(2)*, 190-200.

Gardiner,B.,D.Jamb,R.L.Pitter,J.Hallett, and C. P. R. Saunders (1985), Measurements of initial potential gradient and particles charges in a Montana summer thunderstorm, *J. Geophys. Res.*, *90*, 6079-6086.

Guo Fengxia, Zhang Yijun, Qie Xiushu, et al. (2003) Numerical Simulation of Different Charge Structures in Thunderstorm, *Plateau Meteorology*, *22(3)*, 268-274.

Guo, X.L., Huang, M.Y., 2002. Hail formation and growth in a 3D cloud model with hail-bin microphysics.Atmos. Res. 63, 59– 99.

Helsdon, J.H. and Farley, R., and H. D. Orville (1987), A numerical modeling study of Montana thunderstorm, *J. Geophys. Res., 92,* 5661-5675.

Jayaratne, E. R., C. P. R.Saunders and J. Hallett (1983), Laboratory studies of the charging of soft-hail during ice crystal interactions, *Quarterly Journal of the Royal Meteorological Society*, *109(461),* 609-630.

Kasemir,H.W (1960)., A contribution to the electrostatic theory of a lightning discharge, *J. Geophys. Res., 65*, 1873-1878.

Krehbiel P. R et al. (1999), Three dimensional lightning mapping observations during MEaPRS in central Oklahoma[C]. Proccedings 11th Intn 1. Conf. Atmospheric Electricity, Guntersville, Alabama, June

MacGorman,D.R., J.M.Straka, and C.L.Ziegler (2001), A lightning parameterization for numerical cloud models, *J. Appl. Meteorol., 40*, 459-478.

Mansell ER, McGorman D.R, Ziegler C.L, et al (2002), Simulated three-dimensional branChed lightning in a numerical thunderstorms model. *J. Geophys. Res., 107*(D9), 4075, doi:10.1029/2000JD000244.

Mansell E. R., MacGorman D.R. and Conrad L. Ziegler (2005), Charge structure and lightning sensitivity in a simulated multicell thunderstorm, *J. Geophys. Res.*, *110*, D12100-D12101.

Marshall, T.C.,M.P.McCarthy, and W.D.Rust (1995), Electric field magnitudes and lightning initiation in thunderstorms, *J. Geophys. Res., 100,* 7097-7103.

Pereyra,R.G,E.E.Avila,N.E.Catellano and C.P.R.Saunders (2000), A laboratory study of graupel charging, *J. Geophys. Res.*, *105*, 20803-20812.

Rawlins, F. (1981), A numerical study of thunderstorm electrification using a 3D model inCorporating the ice phase, *Quart. J, R. Met. Soc.*, *108,* 779-800.

Saunders, C. P. R., W. D. Keith, and R. P. Mitzeva (1991), The effect of liquid water on thunderstorm charging, *J. Geophys. Res., 96,* 11,007-11,017.

Saunders, C. P. R., and S. L. Peck (1998), Laboratory studies of the influence of the rime accretion rate on charge transfer during crystal/graupel collisions, *J. Geophys. Res., 103,* 13,949-13,956.

Scott, W.D., and Z. Levin (1975), A stochastic electrical model of an infinite cloud: Charge generation and precipitation development, *J. Atmos. Sci., 32*, 1814-1828.

Stolzenburg M. (1996), An observational study of electrical structure in convective regions of meso-scale convective systems [D] . Ph. D. Diss. Norman : Univ of Oklahoma , *137*

Sun Anping, Yan Muhong, Zhang Yijun, et al. (2002), Numerical study of thunderstorm electrification with a three-dimensional dynamics and electrification coupled model I:Model description and parameterization of electrical process, *Quarterly Journal of Meteorology, 60(6),* 722-731.

Sun Anping, Yan Muhong, Zhang Yijun, et al. (2002), Numerical study of Thunderstorm electrification with a three-dimensional dynamics and electrification coupled model II:Mechanism of electrical structure, *Quarterly Journal of Meteorology, 60 (6)*, 732-739.

Tan Y B ,Tao S C ,Zhu B Y, et al. (2007), A simulation of the effects of intra2cloud lightning discharges on the charges and electrostatic potential distributions in a thundercloud. *Chinese J . Geophys*. (in Chinese) , *50 (4),* 1053～1065.

Takahashi T (1978), Riming electrification as a charge generation mechanism in thunderstorms. *J. Atmos Sci.*, *35*, 1536-1548.

Takahashi T., Miyawaki K. (1984), Reexamination of Riming Electrification in a Wind Tunnel, *J. Atmos. Sci., 59,* 1018-1024.

Takahashi T. (1984), Thunderstorm Electrification – A numerical study, *J. Atmos. Sci., 41,* 2541-2558.

Yan Muhong, Liu xinsheng, An Xuemin, et al. (1996), A simulation study of noninductive charging mechanism thunderstorm I: Affect of cloud factor, *Plateau Meteorology*, *15 (4)* , 425-437.

Yan Muhong, Liu Xinsheng, An Xuemin, et al. (1996d), A simulation study of noninductive charging mechanism in thunderstorm II.Affect of environmental factor, *Plateau Meteorology, 15(4),* 438-447.

Zhang Yijun, Yan Muhong, Liu Xinsheng (1999), A modeling study on discharge process in thundstorm, *Chinese ScienCe Bulletin (in Chinese)*, *44*.

Ziegler, C., MacGorman, D., Dye, J., Ray, P. (1989), A model evaluation of noninductive graupel-ice charing in the early electrification of a mountain thunderstorm, *J. Geophys. Res., 96,* 12,833-12,855

Ziv, A., and Z.Levin (1974), Thundercloud electrification : Cloud growth and electrical development, *J. Atmos. Sci., 31,* 1652-1661.